State Estimation in Power Distribution Systems

by

Côme Carquex

A thesis
presented to the University of Waterloo
in fulfillment of the
thesis requirement for the degree of
Master of Applied Science
in
Electrical and Computer Engineering

Waterloo, Ontario, Canada, 2017

I hereby declare that I am the sole author of this thesis. This is a true copy of the thesis, including any required final revisions, as accepted by my examiners.

I understand that my thesis may be made electronically available to the public.

Abstract

State estimation in power distribution systems is a key component for increased reliability and optimal system performance. Well understood in transmission systems, state estimation is now an area of active research in distribution networks. While several snapshot-based approaches have been used to solve this problem, few solutions have been proposed in a dynamic framework.

In this thesis, a Past-Aware State Estimation (PASE) method is proposed for distribution systems that takes previous estimates into account to improve the accuracy of the current one, using an Ensemble Kalman Filter. Fewer phasor measurements units (PMU) are needed to achieve the same estimation error target than snapshot-based methods. Contrary to current methods, the proposed solution does not embed power flow equations into the estimator. A theoretical formulation is presented to compute a priori the advantages of the proposed method vis-a-vis the state-of-the-art. The proposed approach is validated considering the 33-bus distribution system and using power consumption traces from real households. Engineering insights are presented highlighting the major trade-offs in the choice of decision variables (number of PMUs, PMU accuracy, estimation time-step - i.e. elapsed time between two consecutive estimations) for the LDC: using a smaller time-step allows the LDC to relax the requirements on the PMU quality and their number.

Acknowledgements

I would like to thank my supervisor Professor Catherine Rosenberg for her guidance and insightful advice.

I would also like to thank Professor Kankar Bhattacharya for his consultation and help.

I would like to thank Professor John Simpson-Porco and Professor Claudio Cañizares for their comments on the thesis.

Table of Contents

List of Tables

List of Figures

List of Abbreviations

ARMSEV Average Root Mean Square Error of the Voltage

DSSE Distribution System State Estimation

EnKF Ensemble Kalman Filter

LDC Local Distribution Company

PASE Past Aware State Estimation

PDF Probability Density Function

PMU Phasor Measurement Unit

SCADA Supervisory Control and Data Acquisition system

SoA State of the Art

WLS Weighted Least Squares

List of Symbols

D A $2|I| \times L$ observation ensemble.

$J(\cdot)$ The objective function minimized in the SoA method.

$L_i^p(t)$ The instantaneous active aggregated power at bus i and time t.

$L_i^q(t)$ The instantaneous reactive aggregated power at bus i and time t.

L The ensemble size.

M The $|I| \times |I|$ distribution load flow matrix.

Ψ A $2|I| \times 2|I|$ transition matrix.

Σ A $M \times M$ covariance matrix.

X^k The ensemble of size $2|I| \times L$, at step k.

D A $2|I| \times L$ observation ensemble.

b The scale of a Laplace distribution.

$\Delta T'$ Elapsed time between two forecasts.

ΔT Time-step of the computational timescale.

$\boldsymbol{d}$ A $2|I| \times 1$ observation vector.

$e_i(t)$ Forecast error at bus i and time t.

$\boldsymbol{\epsilon}$ A $2|I| \times 1$ noise vector.

$\boldsymbol{\eta}$ A $M \times 1$ noise vector.

$f(\cdot)$ A function mapping a state vector to a measurement vector.

$h(\cdot)$ A function returning the power-flow solution.

$\mathscr{S}$ PMU placement map.

$\boldsymbol{n}$ A $2|I| \times 1$ noise vector.

B Set of branches defining the connections between buses.

I Set of buses, of cardinality $|I|$.

S Set of buses equipped with a PMU, of cardinality $|S|$.

σ_m^2 The variance of the mth measurement in the measurement vector.

$\boldsymbol{u}$ A $M \times 1$ vector of measurements.

$\boldsymbol{w}$ State vector representing the state of the system using voltage phasors at each bus.

$\boldsymbol{\xi}$ A $2|I| \times 1$ noise vector.

$\boldsymbol{x}$ State vector representing the state of the system using the active and reactive power injected at each bus.

$\boldsymbol{y}$ State vector representing the state of the system using the voltage magnitude and angle at each bus.

$\boldsymbol{z}$ A $2|I| \times 1$ observation vector.

Chapter 1

Introduction

1.1 Motivation

Traditionally, electric power distribution systems have been designed and operated as passive systems to meet the customers' demand. However, with transformation of the grid to a smart grid, the reliability and operational challenges of distribution systems have increased. An operator will need to manage the distribution system more closely in the future, requiring improved visibility of its states [21, 32, 17] which will involve real-time monitoring [5]. Indeed, most solutions to smart grid related challenges at the distribution level assume a knowledge of the states of the system, and therefore essentially rely on Distribution System State Estimation (DSSE), which is a key function of supervisory control that some utilities have already began rolling-out [8].

The state of a power system can be completely defined from the knowledge of all bus voltage magnitudes and angles at time t [20]; typically, state estimation is carried out based on measurements of variables such as the voltage magnitudes and angles, available from Phasor Measurement Units (PMUs). In a snapshot-based context where the state at time t is computed independently of the estimates at times anterior to t, and where the measurement error is additive white Gaussian noise, the weighted least square WLS objective function provides the best performance possible (excluding ill-conditioned cases)[28]. Such an estimator is referred to as the State of the Art (SoA) in this thesis, for the purpose of comparison.

1.2 Problem statement

State estimation of power systems is a well understood problem at the transmission level and is traditionally solved using a snapshot-based WLS method which relies on high quality measurement data from PMUs [20]. However, transmission systems generally have a limited number of buses and are equipped with many measurement devices since it is important to precisely monitor and control the system at all times. On the other hand, distribution systems comprise a large number of buses with little to no measurements available.

While several recent studies have focused on developing low-cost, easy to deploy PMUs [31, 24, 35], it is not practical to install PMUs at every distribution bus. If PMUs were to be placed at selected buses only, there would be infinitely many solutions to the DSSE problem. In order to reduce the number of possible solutions, pseudo-measurements can be used [12], which are load forecasts computed ahead of time to aid DSSE in finding a "good" solution. Typically, a pseudo-measurement at a given load bus comprises an estimate of the expected active and reactive power consumptions at the bus. Load forecasting at the distribution level is difficult, hence pseudo-measurements are usually of poor quality.

These fundamental differences, and the need for affordable solutions, mean that new state estimation approaches are needed for distribution systems. In this thesis, a past-aware method for DSSE, named PASE (Past-Aware State Estimation), where the estimate at time t depends on anterior estimates and based on the Ensemble Kalman Filter (EnKF) [11] is presented.

1.3 Literature review

In transmission systems, the state of the network is typically estimated by using a snapshot approach, based on a weighted least square objective function. This means that at a given time t, the computations are performed independently of previous estimates. The SoA, which is based on WLS, is detailed in Section 2.3 (page 18). Many studies have extended the WLS approach from transmission to distribution systems. A thorough review of literature on the different state estimation techniques and their application to DSSE problems is presented in [23]. Selected papers are discussed in this section.

Snapshot based approaches

Ghosh *et al.* [14] propose a state estimation method for distribution system based on pseudo-measurements that can incorporate telemetered measurements. A probabilistic

approach is used to accommodate pseudo-measurements. Real-time measurements are added as constraints on the probabilistic model.

Baran *et al.* [9] use state estimation based on pseudo-measurements and a WLS objective function, coupled with current measurements to refine loads forecast in distribution systems.

Several papers use a linear formulation of the power-flow equations to make the computations easier. In [26], the power-flow equations were linearized using the first iteration of the backward-forward sweep and a computationally friendly solution method was proposed based on Bayesian inference, which ultimately minimizes a WLS objective function. The authors also showed that PMUs are needed for accurate state estimation, instead of simple voltage magnitude measurements. Using a similar ideas, Arefi *et al.* [7] presented a state estimator based on conditional multivariate complex Gaussian distribution. The state is estimated using conditional probabilities on the Gaussian distributions. Finally Haughton *et al.* presented in [15] a linear state estimation formulation for distribution system. A three-phase linear formulation of the power-flow equations is proposed were the power-flow equations are linearized using partial derivatives.

Compressed sensing theory was used for state estimation with sparse measurements by Alam *et al.* in [3]. The approach proposed uses measurement correlation in time and space to compensate for missing samples. The state reconstruction algorithm is directly embedded into the power-flow equations which makes it very efficient. However, it is not specified how PMU accuracy impacts the algorithm.

In [33], Wang *et al.* used line-current magnitudes and angles as state variables, which varies from typical voltage magnitude and angle measurements state vectors. A traditional WLS objective function is minimized; the different state vector used impose a different linearization process for solving the problem. This approach allows an easier problem formulation when branch current measurements are available.

Klauber *et al.* [19] proposes a semi-definite programming approach to solve the WLS objective function. A convex relaxation of the power-flow equations is proposed. When solving the DSSE, such convex formulation avoids the convergence issues of iterative methods while minimizing the WLS objective function.

Finally, a comparison of some snapshot-based DSSE approaches was presented in [28]. One of the main conclusion of the paper is that the choice of the norm in the objective function (L2 norm for WLS) depends on the probability distribution of the measurement error; a L2 norm being optimal for Normally distributed noise and a L1 norm for Laplace distributed error.

Overall, all the snapshot based approaches solve a similar objective function. They do so in different ways based on the assumptions made. However, given the same inputs, they globally all yield similar estimation errors.

Kalman filter based approaches

Several researchers have used Kalman filters in state estimation problems for transmission systems. An overview is presented in [13]. However, in distribution systems, the poor quality of the pseudo-measurements [27] renders such methods ineffective. Therefore, very few Kalman filtering based methods have been developed for DSSE and none improve over WLS.

Huang *et al.* compared the extended Kalman filter to the unscented Kalman filter in [16]. From the reported results it was noted that there was no visible improvement in performance of the Kalman filter based methods over WLS.

In [25] the impact of choice of the model and measurement covariance matrix on the performance of the extended Kalman filter was examined. It was noted from the results that the proposed filtering approach did not result in any performance improvement.

The above discussed Kalman filter based approaches apply the methods directly from transmission to distribution systems. The problem of poor quality of pseudo-measurements is alleviated by assuming that measurements are available at every bus in real-time or quasi-real-time, usually from synchronized smart-meters, which is not realistic.

1.4 Challenges

Applying the EnKF to this problem is non-trivial, since measurements from sources with different time-scales must be merged. Contrary to WLS and other approaches using different variations of the Kalman filter, PASE does not embed the power flow equations into the estimator, making it a versatile technique. Instead it relies on an external power-flow solver, which is left to the choice of the operator.

1.5 Contributions

Specifically, the contributions of the work are fourfold:

1. A simple characterization of the aggregate load changes at a distribution transformer is proposed, using fine grained consumption data from 20 homes. A method for deriving such characterization based on any dataset is described as well.

2. A maiden attempt is made to apply EnKF to a distribution system sparsely monitored by PMUs for state estimation.

3. An analytical framework is developed to evaluate the performance of PASE.

4. The theoretical results are validated via extensive simulations on a 33-bus distribution system and using power consumption traces from real households. The performances of the proposed PASE approach and WLS are compared and engineering insights are provided to understand the impact of each decision variable on the performance of PASE, as well as the trade-offs to make.

Based on the above discussions, the main message of this work is that PASE is the first technique to improve upon the SoA. It does so significantly when the elapsed time between two consecutive state computations is small (less than 15 minutes), i.e., less PMUs are needed to achieve the same estimation error. This approach to DSSE can help local distribution companies (LDCs) to reduce the number of PMUs required to achieve a similar estimation accuracy as that of the SoA. On the 33-bus distribution system, for a target estimation error of $4e^{-3}$ p.u. on the root mean squared voltage error, the number of PMUs required is divided by 3 compared to the SoA, when computing state estimations 6 seconds apart.

1.6 Outline

The thesis is organized as follows.

Chapter 2 first gives background on power distribution systems and the different timescales involved. The linear Kalman filter and the ensemble Kalman filter are described, as well as two different formulations of the power-flow equations. After providing background information, the relevant literature on DSSE is reviewed. Relevant papers are grouped based on whether they present a snapshot-based approach or a filter-based method. Following on the literature review, the system model considered and the assumptions made are then stated. Finally the SoA method and its WLS objective function are described.

Chapter 3 first describes the load evolution model used by PASE in the EnKF. A method explaining how to build a load model from any dataset is presented. Each of the steps involved in the EnKF computations are then described.

A theoretical formulation for estimating the performance gain achieved by EnKF over WLS is presented. Such formulation alleviate the need for expensive numerical simulations.

Finally, PASE is validated by simulating on the 33-bus system and compared to WLS. A smaller number of PMUs are required to achieve the same estimation error as WLS provided that the system state is computed often (less than 15 minutes apart between two estimations). Engineering insights are provided regarding the trade-offs to be made between the number of PMUs, their accuracy and the timescale chosen. By doing state estimation computation more often, it is possible to relax the requirements on the PMU accuracy or their number without any degradation in the state estimation performance.

Chapter 4 reviews conclusions drawn from the comparison of PASE to WLS and the trade-offs involved. Avenues for future work are then listed, by relaxing some assumptions made in this work.

Chapter 2

Background and Prior Work

Summary

In this chapter, background on distribution power systems and the ensemble Kalman filter is introduced. The system model considered is defined. The SoA method considered for DSSE is presented.

2.1 Background

2.1.1 Distribution Power System

Distribution systems are the link between the transmission system and the end-users. While electricity travels in transmission lines at a high voltage, end-users consume electricity at a low voltage. It is the role of the distribution system to bring electricity to the consumer at a safe voltage. Today, most of the electricity consumed is produced by power plants. At the generation station, the voltage is increased by step-up transformers and the electrical energy is carried over long distances by transmission lines. A high voltage is used in order to minimize energy losses. Transmission lines feed sub-transmission networks, where the voltage is lowered by a step down transformer. A sub-transmission network serves several local distribution substations, located close to centers of demand. The distribution substation represents the beginning of a distribution system; the voltage is lowered by the substation transformer, to which primary feeders are connected.

A radial topology is the most widely used configuration for distribution networks. It is the least expensive, allows a relatively simple operation of the system and an easy expan-

sion of the network. At a given time, there is only one path for the power to flow from the substation to the consumer. Customers with various power and voltage needs are served by the feeders. Each connection to a feeder is called a bus. Typically, loads are classified based on the customer type. Four categories are usually used: residential, commercial, industrial and agricultural. Other load classifications exist, such as geographical location for example (downtown, urban, suburban, rural). Distribution transformers connected to primary feeders lower the voltage even further; they principally serve residential and commercial areas. The low voltage side of distribution transformers represents the secondary network. In North America, distribution transformers are easy to spot as they are often visible from the street; indeed most of them are pole-mounted or pad-mounted. A typical transmission and distribution structure with the corresponding voltage levels is illustrated by Figure 2.1. Voltage levels may vary depending on the region considered .

Along the feeders are often encountered several pieces of equipment that allow safe and reliable operation of the distribution system. Examples of such equipment includes voltage regulators, which are essentially adjustable transformers used to regulate the voltage level of the feeders. Voltage regulator are often found in substation transformers, which have a tap changer on the low voltage side. Reactive power compensation equipments are often used to improve the system power factor and control the voltage. Capacitor banks and reactors are typically used for this purpose. Finally surge protection system, such as surge arrestor, which protect the system from lightning and transient voltage waves from damaging insulations, are commonly found in distribution systems.

2.1.2 Measurements in Distribution Systems

Measurement types

Grid sensing and monitoring is widespread at the transmission level. Supervisory control and data acquisition (SCADA) systems rely on real-time PMU and power measurements to control the network. Such measurements are usually available down to substations. At the consumer level, smart-meters report periodically energy consumption data to local distribution companies. Such information is typically used for billing. At the distribution level however, very little measurement exists, which renders observation of the system difficult. As mentioned in the introduction, several recent studies have focused on developing low-cost, easy to deploy PMUs for distribution networks [31, 24, 35]. Such instruments, when placed into distribution system, would allow better grid sensing and monitoring. Pseudo-measurements are often used as an alternative to scarce “real” measurements. Pseudo-measurements are load forecasts, computed based on historical data. Pseudo-measurements

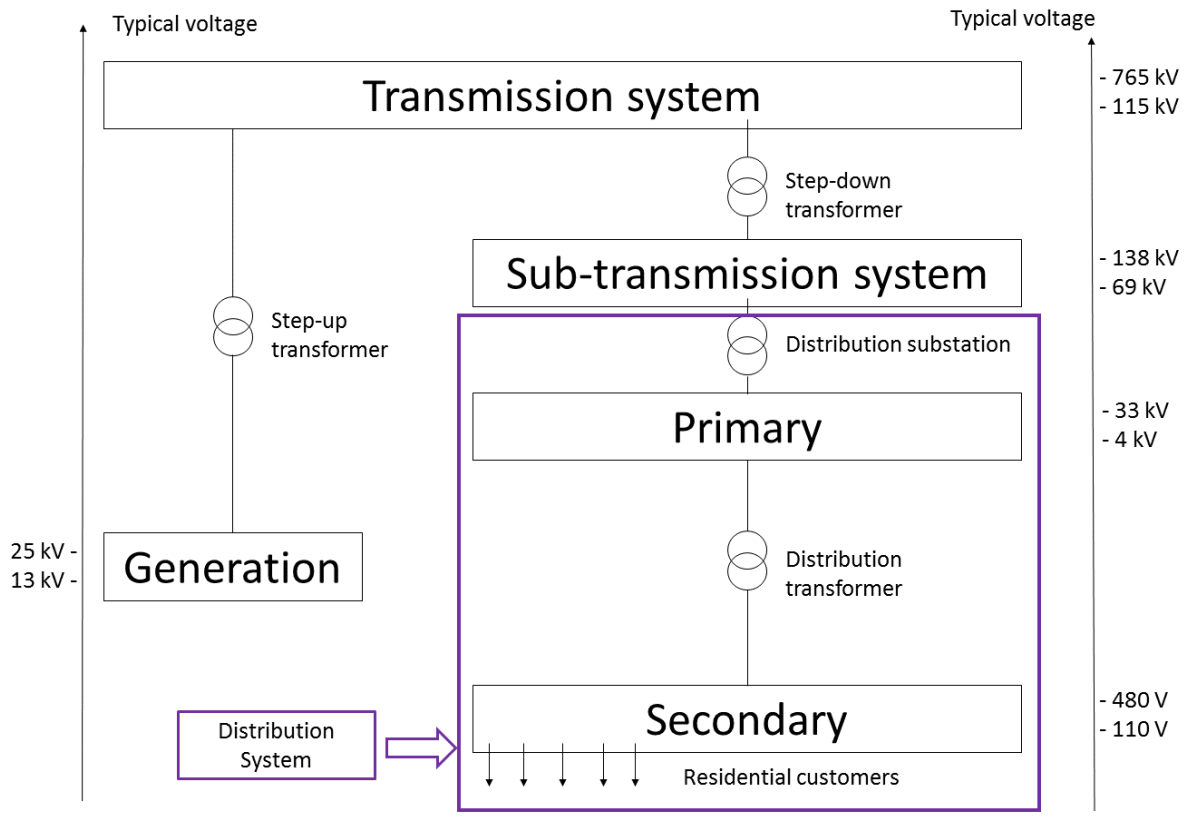

Figure 2.1: Typical transmission and distribution structure with the corresponding voltage levels.

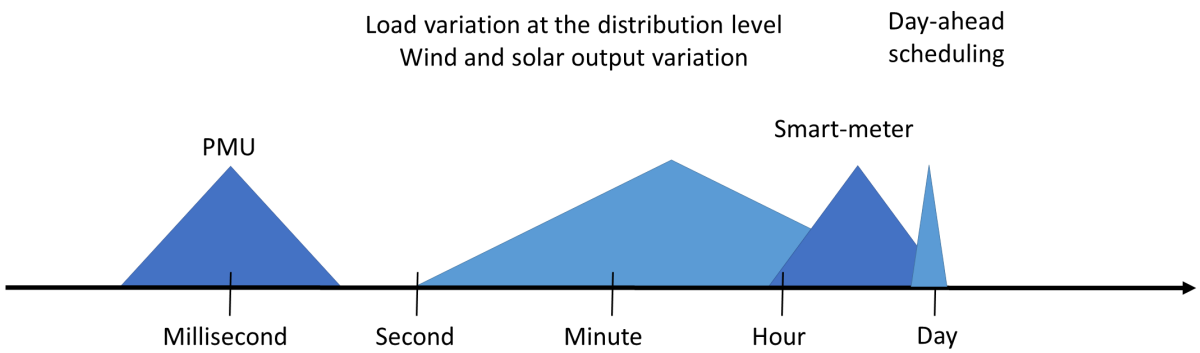

Figure 2.2: Overview of the different time scales in distribution systems. Inspired by Jeff Taft, Cisco

represent a statistical load estimation. Typically, a pseudo-measurement at a given load bus comprises an estimate of the expected active and reactive power consumptions at the bus. Load forecasting at the distribution level is difficult, hence pseudo-measurements are usually of poor quality [27].

Measurement timescales

Several timescales coexist in distribution systems. They are illustrated by Figure 2.2. On one hand, PMUs are capable of producing a measurement of the voltage magnitude and angle at a given bus several times per seconds. On the other hand, load forecasts at the distribution level are usually computed daily, for the next day. In the middle sits smart-meters, which record electric energy consumption periodically, typically in intervals of around 15 minutes to an hour. They communicate that information to the utility daily, but not necessarily at the end of each time interval[1]. Such variety of timescales makes distribution system state estimation challenging.

2.1.3 Power-Flow Equations[2]

Power-flow equations relate bus power injections to the voltage angle and magnitude at each bus of a power system. Power lines impedance need to be known in order to perform

[1]New generations of smart-meters, which will be rolled out in the future, will have a finer-grained timescale.

[2]Variable names used in this sub-section are dummies corresponding to typical names.

the computations. Given that at the distribution voltage level the line shunt capacitance is small, its value will be neglected. The branch impedance between two buses i and k ($i \neq k$) is denoted by $z_{ik} = r_{ik} + jx_{ik}$, where r_{ik} represents the resistance of the line and x_{ik} its reactance. The term z_i denotes the admittance-to-ground at bus i. Let I be the set of all buses, with cardinality $|I|$, of a distribution system. One can represent the topology as well as the line characteristics of such system using a nodal admittance matrix, typically named Y; Y is an $|I| \times |I|$ matrix defined as follow:

$$Y_{ik} = \begin{cases} \frac{1}{z_i} + \Sigma_{\substack{j=1,\cdots,|I| \\ j \neq k}} \frac{1}{z_{ij}} & \text{if } i = k \\ \frac{-1}{z_{ik}} & \text{if } i \neq k \end{cases} \tag{2.1}$$

A three-phase radial distribution system assumed to be balanced can be represented by an equivalent single-line diagram as illustrated in Figure 2.3. In a radial distribution system, a main feeder is connected to a single power source: the substation. The substation bus is referred to as the slack bus, and represents a reference voltage source of magnitude V_0. Several formulations of the power-flow equations exists. The typical load flow equations and the backward-forward sweep method are presented in this section. Other methods more advanced exist such as harmonic solvers, used by openDSS [2] for example.

Distribution Load Flow Equations

Assuming that the loads at a given bus i are power sinks (i.e. the power flows from the bus to the load) denoted by $S_i = P_i + jQ_i$, the load flow equations are expressed as follow:

$$P_i = -\Sigma_j V_i V_j |Y_{ij}| cos(\theta_{ij} + \delta_j - \delta_i) \qquad \forall i \neq \text{slack} \tag{2.2}$$

$$Q_i = \Sigma_j V_i V_j |Y_{ij}| sin(\theta_{ij} + \delta_j - \delta_i) \qquad \forall i \neq \text{slack} \tag{2.3}$$

where $\theta_{ij} = \angle Y_{ij}$. V_i and δ_i represents the voltage magnitude and angle at bus i. Note that typically in transmission, the power at a bus is expressed in term of injected power (i.e. the power flows from the bus to the network), in which case the right-hand side of the equations should be multiplied by -1.

The power-flow equations are such that given V_i and δ_i at each bus, it is straightforward to compute P_i and Q_i. However, the opposite is not true and one has to solve a set of non-linear equations to compute the voltage knowing only power consumptions. This can be achieved using well known methods such as Newton-Raphson or Gauss-Seidel [20].

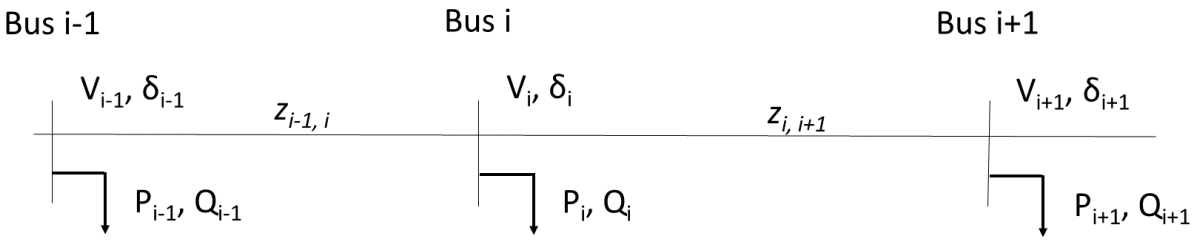

Figure 2.3: Single line diagram of a distribution feeder

Backward-Forward Sweep

The backward-forward sweep is a method well suited for solving power-flows in distribution systems. It is an iterative methods, that typically converges within a few iterations. A vectorized formulation is obtained by using a distribution load flow matrix M, as described in [30]. The construction of M based on lines impedance is not repeated here as it is straightforward. One iteration of the backward-forward sweep at step j is given as:

$$\begin{bmatrix} \underline{v}_1^j \\ \vdots \\ \underline{v}_{|I|}^j \end{bmatrix} = \begin{bmatrix} V_0 \\ \vdots \\ V_0 \end{bmatrix} - M \times \begin{bmatrix} \overline{S}_1/\underline{v}_1^{j-1} \\ \vdots \\ \overline{S}_{|I|}/\underline{v}_{|I|}^{j-1} \end{bmatrix} \tag{2.4}$$

where $\underline{v}_i^j$ is the estimated voltage at bus i and iteration j, S_i is the power consumed at bus i ($S_i = P_i + jQ_i$) and $\overline{S}_i$ the conjugate of S_i. Note that if S_i was referring to the injected power at bus i instead, the subtraction would become and addition in (2.4). The complete algorithm is given by Algorithm (1). At a given step j, the vector $\boldsymbol{w}^j$ is defined as:

$$\boldsymbol{w}^j = \begin{bmatrix} \underline{v}_1^j \\ \vdots \\ \underline{v}_{|I|}^j \end{bmatrix} \tag{2.5}$$

A flat voltage profile is usually chosen for the first iteration ($j = 0$), meaning that for each bus i, $v_i^0 = V_0$. The algorithm stops when the computed voltage between two iterations change by less than a predefined threshold.

Algorithm 1 Backward-forward sweep algorithm

Input: S_i $(\forall i \in I)$, M, ϵ

Initialize $\underline{v}_i^0 = V_0$, $(\forall i \in I)$

repeat

  Compute $\boldsymbol{w}^j$ using $\boldsymbol{w}^{j-1}$ and eq. (2.4)

until $||\boldsymbol{w}^j - \boldsymbol{w}^{j-1}|| < \epsilon$

Output: voltage profile: $\boldsymbol{w}$

2.1.4 Kalman Filters[3]

The Kalman filter is a sequential data assimilation method, which provides an estimate of the state of the system by combining information from a model and observations from the system using Bayesian inference. The linear Kalman filter [18] and the ensemble Kalman filter [11] fundamentals are reviewed in this section as they will both be used later on in the thesis.

Linear Kalman Filter

The linear Kalman filter can be used with linear models of the system dynamics and observations. Each iteration of the Kalman filter is a two-steps process:

1. **Prediction step**: based on the state estimated at the previous iteration and the system model, the filter predicts the current system state, along with its uncertainty.
2. **Update step**: using the observed measurements for the current iteration and their uncertainties, the state prediction is refined and updated, using a weighted average.

The idea behind the Kalman filter is simple: the additional information provided by the model allows to compute a better estimate of the system state instead of relying only on measurements. The Kalman filter model assumes that the system state at time k is an evolution from the state at time $(k-1)$ such that:

$$\boldsymbol{x}_k = F\boldsymbol{x}_{k-1} + \boldsymbol{\epsilon}_k \tag{2.6}$$

[3]Variable names used in this sub-section are dummies corresponding to typical names.

where $\boldsymbol{x}_k$ is the system state at time k, F is the system evolution model that is assumed to be known and $\boldsymbol{\epsilon}_k$ is a vector of random noise with known covariance matrix Q. The measurements are assumed to be modeled such that:

$$\boldsymbol{z}_k = H\boldsymbol{x}_k + \boldsymbol{\eta}_k \tag{2.7}$$

where $\boldsymbol{z}_k$ is the measurement vector at time k, H is the observation model matrix that is assumed to known and $\boldsymbol{\eta}_k$ is a vector that models random noise with known covariance matrix R.

The state of the filter is represented by two variables: $\hat{\boldsymbol{x}}_k$ which is the estimated state at time k and P_k which is the estimated error covariance matrix of the computed state. For each iteration of the filter, the following quantities are computed:

1. **Prediction step**

$$\boldsymbol{x}_k^f = F\hat{\boldsymbol{x}}_{k-1} \tag{2.8}$$
$$P_k^f = FP_{k-1}F^T + Q \tag{2.9}$$

2. **Update step**

$$K_k = P_k^f H^T (HP_k^f H^T + R)^{-1} \tag{2.10}$$
$$\hat{\boldsymbol{x}}_k = \boldsymbol{x}_k^f + K(\boldsymbol{z}_k - H\boldsymbol{x}_k^f) \tag{2.11}$$
$$P_k = P_k^f - K_k H P_k^f \tag{2.12}$$

When the errors corresponds to additive white Gaussian noise, the filter gives the optimal estimate for the system state in the least square sense; indeed it minimizes the following cost function at each iteration (the iteration number is dropped for better readability):

$$J(\boldsymbol{x}) = (\boldsymbol{x} - \boldsymbol{x}^f)^T (P^f)^{-1} (\boldsymbol{x} - \boldsymbol{x}^f) + (\boldsymbol{z} - H\boldsymbol{x})^T R^{-1} (\boldsymbol{z} - H\boldsymbol{x}) \tag{2.13}$$

One shortfall of the linear Kalman filter is that is cannot handle non-linear observations. The ensemble Kalman filter is one possible solutions that addresses this limitation.

Ensemble Kalman Filter (EnKF)

The linear Kalman filter maintains a covariance matrix associated with the state estimate. The EnKF does not use such a matrix and represents the system state probability density

function (pdf) using a set of state vectors called ensemble. Such ensemble at time-step k is named X^k and is given by:

$$X^k = [\boldsymbol{x}_k^1, \cdots, \boldsymbol{x}_k^L] \tag{2.14}$$

where L is the ensemble size and each $\boldsymbol{x}_k^l$ is a member of the ensemble. The two variables that define the state of the filter can be derived from the ensemble. The estimated system state is obtained by computing the mean of the ensemble columns, such that:

$$\hat{\boldsymbol{x}}_k = E[X^k] = \frac{1}{L}\Sigma_{l=1}^{L}\boldsymbol{x}_k^l \tag{2.15}$$

where $\mathrm{E}[A]$ is the mean of the column vectors contained in ensemble A. The covariance matrix of the state estimate is replaced by the empirical covariance computed from the ensemble. The covariance estimator $\mathrm{cov}(A, B)$ of two ensembles A, B is defined as [11]:

$$\mathrm{cov}(A, B) = \frac{1}{N-1}(A - \mathrm{E}[A])(B - \mathrm{E}[B])^T \tag{2.16}$$

For $\mathrm{cov}(A, A)$ the shorter syntax $\mathrm{cov}(A)$ is used. Therefore at iteration k, P_k is computed using the ensemble:

$$P_k = \mathrm{cov}(X^k) \tag{2.17}$$

The size of the ensemble, L, will impact performance. A small ensemble size will yield faster computations. However the covariance estimate from the ensemble will be less accurate. Therefore there is a trade-off between computational speed and accuracy and a typical choice is a size of $L = 500$ or 1000 [11].

Each iteration of the EnKF, like the linear Kalman filter, is a two-steps process and the equations for each steps are very similar:

1. **Prediction step**: at a given iteration k, the predicted ensemble X_f^k is computed by integrating forward in time each vector of the ensemble X^{k-1}, computed at the previous iteration using the system model:

   $$X_f^k = FX^{k-1} + [\boldsymbol{\eta}_1, \cdots, \boldsymbol{\eta}_L] \tag{2.18}$$

   where each $\boldsymbol{\eta}_l$ $(l = 1, \cdots, L)$ is drawn from a known distribution representing the system evolution noise, with covariance Q.

2. **Update step**: a measurement ensemble Z^k is artificially created from the observation vector $\boldsymbol{z}_k$ such that:

   $$Z^k = [\boldsymbol{z}_k + \boldsymbol{\omega}_1, \cdots, \boldsymbol{z}_k + \boldsymbol{\omega}_L] \tag{2.19}$$

   where $\boldsymbol{\omega}_l$ $(l = 1, \cdots, L)$ is a noise vector drawn from a known distribution representing the measurement error, with covariance R. Two cases are considered:

(a) If the measurements can be linearly derived from the system state, the update equations are as follow:

$$K_k = \text{cov}(X_f^k, HX_f^k)[\text{cov}(HX_f^k) + \text{cov}(Z^k)]^{-1} \tag{2.20}$$

$$X^k = X_f^k + K(Z^k - HX_f^k) \tag{2.21}$$

(b) If the measurements are the results of a nonlinear measurement functional $h(\cdot)$, such that $\boldsymbol{z_k} = h(\boldsymbol{x}_k) + \boldsymbol{\kappa}_k$, where $\boldsymbol{\kappa}_k$ is a noise vector, then a slightly different approach is required. A temporary augmented state vector $\tilde{\boldsymbol{x}}_k^l$ and augmented ensemble $\tilde{X}^k$ are defined:

$$\tilde{\boldsymbol{x}}_k^l = [\boldsymbol{x}_k^l, h(\boldsymbol{x}_k^l)]^T \tag{2.22}$$

$$\tilde{X}^k = [\tilde{\boldsymbol{x}}_k^1, \cdots, \tilde{\boldsymbol{x}}_k^L] \tag{2.23}$$

Similarly, a temporary linear observation operator $\tilde{H}$ on the augmented state is defined and is such that:

$$\tilde{H}\begin{pmatrix}\boldsymbol{x}_k^l \\ \boldsymbol{z}_k\end{pmatrix} = \boldsymbol{z}_k \tag{2.24}$$

The update equations are then given by:

$$K_k = \text{cov}(\tilde{X}_f^k, \tilde{H}\tilde{X}_f^k)[\text{cov}(\tilde{H}\tilde{X}_f^k) + \text{cov}(Z^k)]^{-1} \tag{2.25}$$

$$X^k = X_f^k + K(Z - \tilde{H}\tilde{X}_f^k) \tag{2.26}$$

The EnKF is able to handle non-linear measurement and is independent of the way the measurement functional is computed (i.e. only $h(\boldsymbol{x})$ needs to be known and the explicit expression of $h(\cdot)$ is not needed). The EnKF versatility comes however at the cost of higher computations.

2.2 System Model

The assumptions are stated in this section. A three-phase balanced distribution system under normal operations is considered. The DSSE problem is solved by the local distribution company using an appropriate computational platform. The following information is needed to implement DSSE, both with the SoA method and the proposed PASE method.

Computational timescale: a new state estimate is computed every ΔT. Typically in transmission systems, a time-step of 5 to 15 min is considered. In distribution systems

smaller time-steps are needed because of higher load volatility, which can arise for example with high penetration of renewables. The value of ΔT has an impact on the computational burden. In this work time-steps from 6 seconds to 15 minutes are considered. Altogether, the choice of an appropriate timescale for DSSE problems is still an open question.

Topology: the distribution system has a radial topology and is defined by a set of buses I of cardinality $|I|$ as well as a set of branches B of constant and known impedances, connecting the buses. The substation transformer is modeled as a reference voltage source of magnitude V_0.

Measurements: the subset $S \subseteq I$ of buses are equipped with PMUs that monitor every ΔT both the bus voltage magnitudes (V_s) and bus angles (δ_s). The measurements reported by the PMUs are assumed to be unbiased and the variance of the error of the readings is known. These assumptions are commonly made in state estimation works [20]. A broadband communication infrastructure is available to transmit the measurements with low latency and high reliability. The PMUs are placed in the distribution system according to a given mapping $\mathscr{S}$.

Pseudo-measurements: these are forecasts that "measure" both active and reactive powers. They are available for each bus i in I. Forecasts are made at periodic intervals $\Delta T'$, typically once a day for the next day (day-ahead forecast). At the time of computation, the most recent forecast is used. Clearly, forecasts and PMU measurements are on completely different time-scales ($\Delta T' \gg \Delta T$), hence the non-triviality of the EnKF. Forecasts are made based on historical data. Previous estimation work based on Kalman filters assumed real-time consumption data. This strong requirement is relaxed with forecasts.

Data requirements: both the SoA and PASE approaches require a forecasting method as well as sample power consumption traces (active and reactive) from the system at the level of each distribution transformer, from which the forecasting method can be calibrated. Using the data, error parameters can be obtained offline. Let $e_i(t)$ be the forecast error at bus i and time t (for active power, for example); $e_i(t)$ is assumed to be a stationary random process. Moreover, forecasts are assumed to be unbiased ($\mathrm{E}[e_i(t)] = 0$) and the variance of the errors ($\mathrm{E}[e_i(t)^2]$) to be known. The estimation of the variance of the forecast errors comes from the acquired data. The assumption of an unbiased forecast is a strong hypothesis, although it is almost always used by researchers [26].

The proposed PASE method needs two additional information that can be derived from the same sample data: a load evolution model (which will be discussed in Section 3.2, page 22) and the forecast error correlation coefficient, evaluated between two (computation) time-steps at a given bus (i.e., $\mathrm{E}[e_i(t)e_i(t-\Delta T)]$). Given that the data samples are needed for both methods, not much work is involved to derive these additional quantities from it.

Finally, the load forecast errors are assumed to be uncorrelated between buses, an assumption often made in the literature [26]. Note that even if this assumption is not made, the SoA and PASE are still valid. In such a case, the correlations need be taken into account in the computations.

System state: it is represented by state vectors; different (equivalent) state representations may be used depending on their ease of use in the problem formulation. For example,

$$\mathbf{y}[t] = [\mathbf{V}[t]^T, \boldsymbol{\delta}[t]^T]^T$$

is a possible state vector representation, where $\mathbf{V}[t]$ is the vector of voltage magnitudes at each bus, and $\boldsymbol{\delta}[t]$ the vector of voltage angles. Another way is to define $\mathbf{x}[t] = [\mathbf{P}[t]^T, \mathbf{Q}[\mathbf{t}]^T]^T$ where $\mathbf{P}[t]$ and $\mathbf{Q}[t]$ denotes the vectors of active and reactive power injections at each bus, respectively. Note that the power-flow equations link the state-vectors $\mathbf{x}$ and $\mathbf{y}$. A third way, used in theoretical formulations, is $\mathbf{w}[t] = [\underline{v}_1[t], \ldots, \underline{v}_{|I|}[t]]^T$ where $\underline{v}_i[t]$ is the voltage phasor at bus i, time t; this can also similarly be related to other representations.

Limitations: In this work, unbalanced system, distributed generation and biased measurements are not considered and are left for future studies.

2.3 State of the Art

The SoA method [20] used to solve the DSSE problem is a snapshot approach and uses a nonlinear WLS objective function. Voltage magnitude and angle at each bus are used to represent the state of the system; $\mathbf{y}$ is thus used as state vector. Given the system characterized by the sets I, B, S and the mapping $\mathscr{S}$, the system state, at a given time, is estimated using an overdetermined set of equations. In the following, the time dependency of the variables is dropped for better readability. The variables to be determined are the $2|I|$ state variables. Each measurement adds one constraint. There are either 2 or 4 measurements per bus (active/reactive power forecast, voltage magnitude, and angle), depending on whether there is a PMU at the bus. The number of constraints is given by $M = 2|I| + 2|S|$. The PMU measurements and the forecasts are stored in a vector $\mathbf{u}$ of length M, and are related to the system state as per the following model:

$$\mathbf{u} = f(\mathbf{y}) + \boldsymbol{\eta} \tag{2.27}$$

where f is the function that maps the state vector to the measurement vector, and $\boldsymbol{\eta}$ is the vector containing the noise term of each measurement. For example:

$$f(y) = [\mathbf{V}(y)^T, \boldsymbol{\delta}(y)^T, \mathbf{P}(y)^T, \mathbf{Q}(y)^T]^T \tag{2.28}$$

where $\mathbf{V}(y)$ and $\delta(y)$ are the vectors respectively containing the voltage magnitude and angle measurements at the buses with PMUs and $\mathbf{P}(y)$ and $\mathbf{Q}(y)$ are vectors of active and reactive power forecasts of size $|I|$, respectively; $\mathbf{P}(y)$ and $\mathbf{Q}(y)$ can be computed from $\mathbf{y}$ using power-flow equations. Assuming that the measurement errors are uncorrelated and have zero mean, the covariance matrix Σ corresponding to the error vector $\boldsymbol{\eta}$ is written as:

$$\Sigma = \text{diag}(\sigma_1^2, ..., \sigma_M^2) \tag{2.29}$$

where σ_m^2 is the variance of the mth measurement. The objective function to be minimized at each time-step is given below:

$$J(\mathbf{y}) = (\mathbf{u} - f(\mathbf{y}))^T \Sigma^{-1} (\mathbf{u} - f(\mathbf{y})) \tag{2.30}$$

Another common and equivalent formulation is:

$$J(\mathbf{y}) = \Sigma_{m=1}^{M} (\frac{\mathbf{u}_m - f_m(\mathbf{y})}{\sigma_m})^2 \tag{2.31}$$

Several methods exist to minimize the objective function. The most popular ones are the Gauss-Newton method and Newton-Raphson method [20]. The Gauss-Newton method involves the linearization of the vector function $f(\cdot)$ using Taylor expansion. The original minimization problem is transformed into a linear least-square problem, which can be solved using the normal equations [1]. For Newton-Raphson, the optimality conditions are applied directly to the objective function; namely the gradient of the objective function is equated to zero ($\frac{\partial J(\mathbf{y})}{\partial \mathbf{y}} = 0$). The root of the equation is then found using the Newton-Raphson method [20].

Chapter 3

Past-Aware State Estimation

Summary

In this chapter, the proposed method, PASE, is presented. The underlying load evolution model and its derivation process are defined. The application of the ensemble Kalman filter to the state estimation problem is detailed. A theoretical formulation for computing the performance gain of PASE over the SoA is introduced. PASE and the theoretical formulation are validated on the 33-bus distribution system and compared to the SoA. Less PMUs are required to achieve the same estimation error as the SoA. Engineering insights on the impact of three decision variables (number of PMUs, PMU accuracy, estimation time-step) on the estimator performance are given, highlighting the major trade-offs.

To solve the DSSE problem, PASE, an EnKF-based method, is proposed. As mentioned in Section 2.1.4, Kalman filters are sequential filtering methods. Each iteration is a two steps process: 1) the system state is integrated in time using an evolution model, defining an (*a priori*) state estimate. 2) Available measurements (including pseudo-measurements) are used to correct the estimate and define the updated state. The term *assimilation* is used to refer to the second step. Kalman filters rely on a system model. The model used in this approach is a load evolution model and is presented in Section 3.2. The idea behind the proposed approach is simple: the additional information provided by the load evolution model and the previously estimated state is used to alleviate the poor quality of pseudo-measurements.

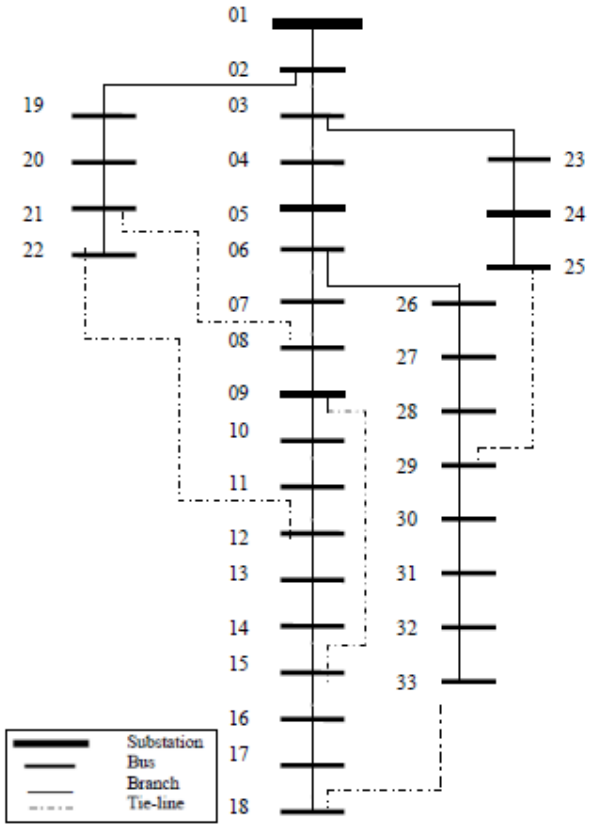

Figure 3.1: Layout of the 33-Bus radial distribution system.

3.1 33-Bus test system

The 33-Bus test feeder will be used for simulation purposes [10]. The 33-Bus feeder is a distribution system. It is balanced and can be represented as a one line diagram; the layout of the system is given Figure 3.1. The feeder parameters are given in Table A.1 page 46. The first bus represents the substation. For each subsequent bus, static load consumption data is given Table A.2 page 47.

3.2 Load evolution model

For each distribution transformer bus, an evolution model for the aggregate load is needed, both for the active and reactive power consumptions. Specifically, the load variation between two (computation) time-steps is considered: let $L_i^p(t)$ and $L_i^q(t)$ denote the instantaneous active and reactive aggregated power respectively, at bus i and time t. It is assumed that $L_i^p(t)$ and $L_i^q(t)$ are stationary random processes. The load variation (aka load evolution model) for active and reactive powers are defined as the stationary random processes $L_i^p(t) - L_i^p(t - \Delta T)$ and $L_i^q(t) - L_i^q(t - \Delta T)$ respectively, characterized by their probability density functions (pdf). The mean of the processes is zero and the variance of the processes can be computed from the pdf both for active and reactive powers at bus i, denoted $(\sigma_i^p)^2$ and $(\sigma_i^q)^2$, respectively. Such an evolution model is simple and fits within the EnKF framework. The pdf can be derived empirically, for example, from the existing required sample traces, discussed in Section 2.2, page 16. Clearly a given load evolution model is valid only for systems with similar load compositions, and will vary for different geographical areas.

The (bus) load evolution model was developed using a fine-grained energy consumption dataset from Ontario, Canada. The dataset used to build the model is described in [6] and comprises instantaneous active power consumption data from 20 homes, collected over eight months, with a resolution of 6 seconds. To the best of the authors' knowledge, very few datasets with such granularity exist in practice. The dataset is split randomly into two subsets, one for deriving the characterization (training set), and one for the validation process (testing set). No distinction is made between the size of the houses nor the time of the year. The resulting dataset is a collection of a few thousands of traces. Although 20 homes may seem to be a limited sample size, considering the daily power traces independently allows to have a large number of unique profiles. Moreover the 20 households cover a wide range of living area sizes and energy consumption patterns which increases the trace diversity.

Let n be the number of households connected to a bus. Using the training set, empirical distributions for load changes were constructed for different values of time-steps ΔT and aggregation levels n. Aggregation levels of more than 20 houses where obtained via bootstrap resampling of the dataset. A Laplace distribution described by a scale parameter b (and variance $\sigma^2 = 2b^2$) was found to be a good fit. Its probability density function (pdf) is given as:

$$pdf(x) = \frac{1}{2b} e^{\frac{-|x|}{b}} \tag{3.1}$$

The mean value is set to zero since as many positive and negative load changes are expected. This implies that the transition model is the identity, while its uncertainty is characterized

by the Laplace distribution. The fit of the distribution is evaluated by comparing the normalized empirical pdf to the Laplace pdf using the total variation distance

$$W = 1/2 \sum_{k=0}^{K-1} |PDF_{Emp}[k] - PDF_{Laplace}[k]| \tag{3.2}$$

where K is the number of points used to build the empirical pdf. The influence of ΔT and n on the distribution variance is illustrated in Fig. 3.2. The variance essentially describes the load variation over time, a small value implying little variations. It is noted that as n increases and ΔT shrinks, the value of σ^2 diminishes. The results indicate that the fit is very good for every aggregation level and time-step considered. The worst fit of all the one considered is illustrated by Figure 3.3. It is still good visually and corresponds to a total variation distance of 0.6.

It was assumed that load changes are uncorrelated between buses; which can be verified to hold true from the dataset, for any value of n and ΔT up to 30 minutes[1].

The values of σ^2 are derived empirically as a function of n and ΔT. They are used to compute the evolution step of the EnKF. Since no reactive power consumption dataset was available, a similar model is assumed for reactive power changes. However, active and reactive power consumption changes are assumed to be independent, which is a common assumption in DSSE literature[2]. The proposed method is generic and can be applied to any dataset from across the globe.

3.3 Ensemble Kalman Filter

Each iteration of the EnKF (corresponding to a computation of the state vector at time-step k) follows the procedure detailed in Algorithm 2, each steps of the algorithm are discussed next.

3.3.1 Initial Ensemble

The state vector $\mathbf{x} = [\mathbf{P}^T, \mathbf{Q}^T]^T$ (of size $2|I|$) is used. It is chosen given that the load evolution model described in Section 3.2 is defined in terms of injected power. The pdf

[1]Even if this assumption is not respected, the EnKF formulation is still valid. In such a case, the correlation need be taken into account in the computations

[2]Even if this assumption is not respected, PASE is still valid. The only difference being that it could perform even better if the dependency was added to the model.

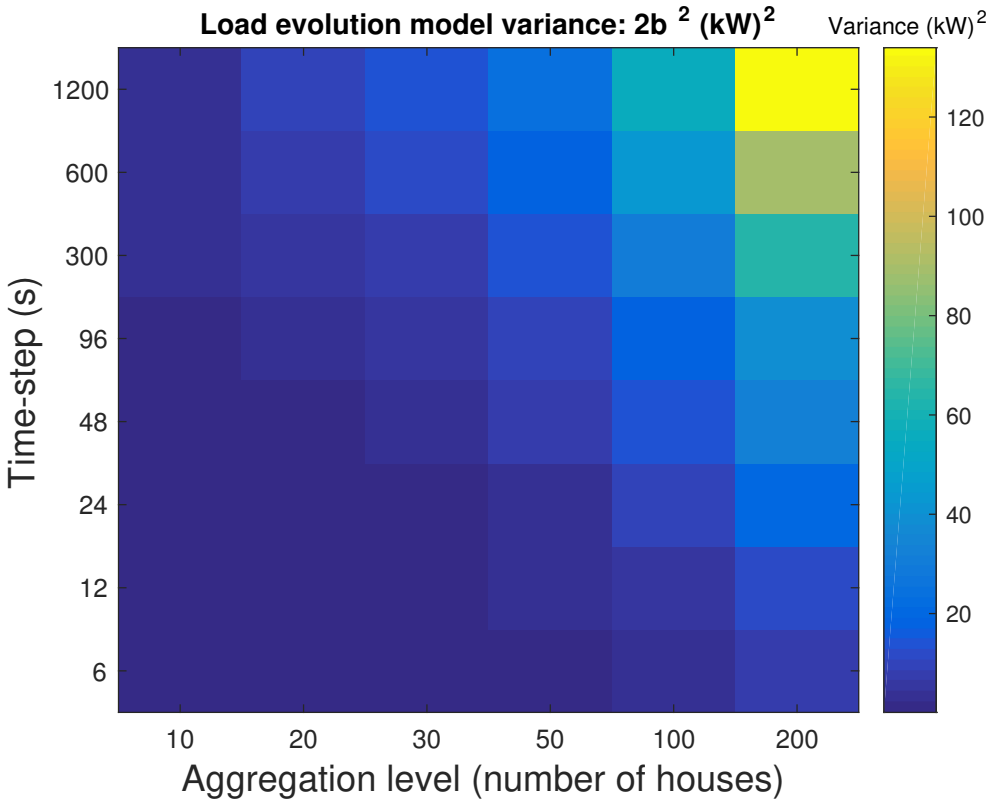

Figure 3.2: Influence of aggregation level and time step on the model variance ($2b^2$). The fit of the Laplace distribution is visually good for all the time-steps and aggregation levels considered here.

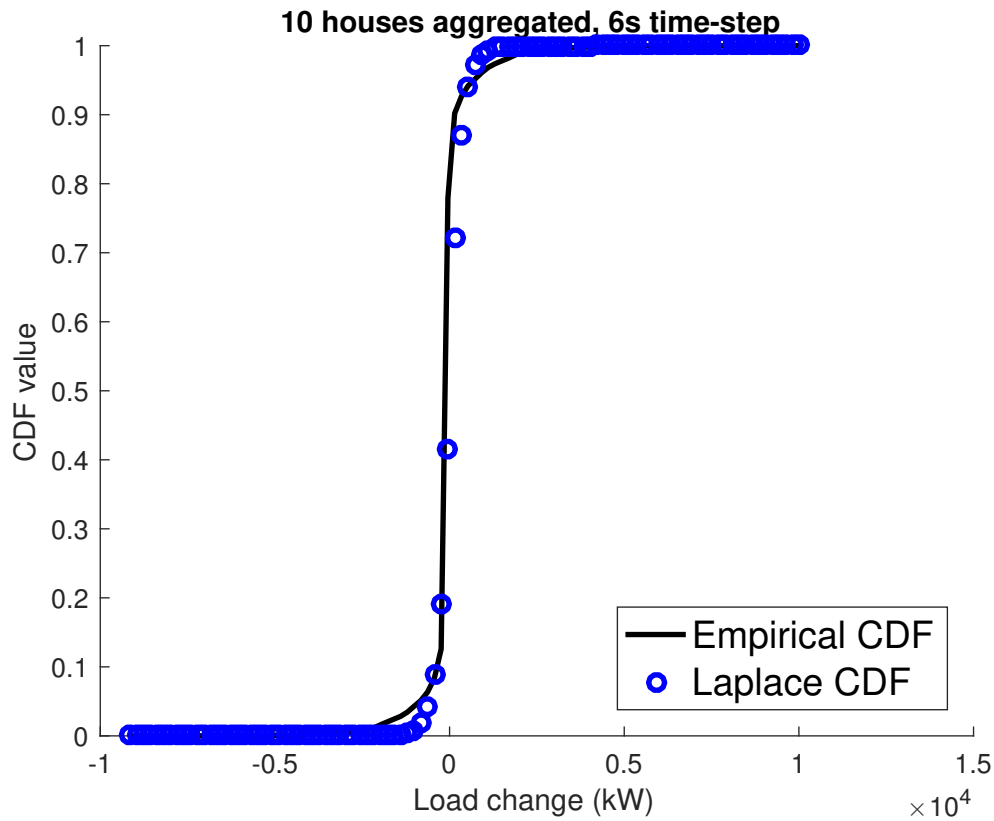

Figure 3.3: Empirical cumulative distribution function of the load changes values and Laplace distribution fit. This illustrates visually the worst fit over all the considered times-steps and aggregation levels.

Algorithm 2 Estimation of the state at time-step k

Input: X^{k-1}, measurements and pseudo-measurements at time-step k.

1: Compute X_p^k: integrate the ensemble in time (Eq. 3.3)
2: Compute X_u^k: assimilate pseudo-measurements (Eq. 3.11)
3: Compute X_a^k: assimilate PMU measurements (Eq. 3.13)
4: $X^k \leftarrow X_u^k$

Output: Estimated state $\tilde{\mathbf{x}}^{\mathbf{k}} = E[X^k]$ for time-step k.

of the state vector $\mathbf{x}$ is represented by an ensemble of size L: $X^0 = [\mathbf{x}_1^0, \ldots, \mathbf{x}_L^0]$, X^0 is a $2|I| \times L$ matrix containing the ensemble members. The initial ensemble is built by choosing a "best-guess" estimate $\mathbf{x}^0$ of the state vector, to which perturbations are added to represent the error statistics of the initial guess. The error distribution chosen for the initial ensemble is discussed in Section 3.5.

3.3.2 Ensemble Integration

The EnKF is considered at time-step k. The prior ensemble X_p^k is obtained by individually integrating forward in time each vector of the ensemble X^{k-1}, which was computed at the previous time-step. The discrete integration is such that:

$$X_p^k = X^{k-1} + [\mathbf{n}_1, \ldots, \mathbf{n}_L] \tag{3.3}$$

where $\mathbf{n}_l$ $(l = 1, \ldots, L)$ are column vectors of size $2|I|$ containing the stochastic noise which accounts for the uncertainties of the load evolution model. Based on the load evolution model defined in Section 3.2, two variance values $(\sigma_i^p)^2$ and $(\sigma_i^q)^2$ are associated to each bus i $(i = 1, \ldots, |I|)$, respectively for the active and reactive powers. Their values depend on the empirical pdf derived. Each $n_{i,l}$ and $n_{|I|+i,l}$ $(i = 1, \ldots, |I|)$ is respectively drawn from a distribution which represents the empirical pdf of the load evolution model. Note that the EnKF can accept any load evolution model.

3.3.3 Assimilation of Pseudo-Measurements

The assimilation of measurements and pseudo-measurements correspond to the update step of the Kalman filter, described at the beginning of Chapter 3, page 20.

An assumption in Kalman filtering is that the measurement error is white Gaussian noise. Since pseudo-measurements are forecasts and do not depend on the state of the system, they do not satisfy this requirement; instead the forecast error is correlated in time. This problem, which is recurrent in Kalman-based kinematic GPS applications has been solved previously, and a summary of the different existing techniques can be found in [34]. The solution chosen is the time-differencing approach described in [22] to remove time-correlated error in the pseudo-measurements. This method was selected for two reasons: 1) it does not require any reinterpretation of the Kalman equations and 2) it does not introduce any latency.

To remove the correlations, the following process is used. Let the transition matrix Ψ of the time-correlated error be defined as:

$$\Psi = \text{diag}(\psi_1^p, \ldots, \psi_{|I|}^p, \psi_1^q, \ldots, \psi_{|I|}^q) \tag{3.4}$$

where ψ_i^p and ψ_i^q $(i = 1, \ldots, |I|)$ are the forecast error correlation coefficients at bus i, respectively for active and reactive powers, introduced in Section 2.2; Ψ is diagonal since the forecast errors between buses are assumed to be uncorrelated. Q is defined as the model noise covariance matrix, and is given as:

$$Q = \text{diag}((\sigma_1^p)^2, \ldots, (\sigma_{|I|}^p)^2, (\sigma_{|I|+1}^q)^2, \ldots, (\sigma_{2|I|}^q)^2) \tag{3.5}$$

R is the covariance matrix of the forecast error, of size $2|I| \times 2|I|$. R is diagonal since the forecast errors are assumed not correlated across buses, and is given as:

$$R = \text{diag}((\sigma_1^{fp})^2, \ldots, (\sigma_{|I|}^{fp})^2, (\sigma_{|I|+1}^{fq})^2, \ldots, (\sigma_{2|I|}^{fq})^2) \tag{3.6}$$

where σ_i^{fp} and σ_i^{fq} are the standard deviations of the forecast error at bus i, respectively for the active and reactive powers. The pseudo measurements are contained in a vector $\mathbf{d}$ of size $2|I|$. An ensemble D of L perturbed observations is defined such that $D = [\mathbf{d}_1, \ldots, \mathbf{d}_L]$ with each $\mathbf{d}_l = \mathbf{d} + \boldsymbol{\epsilon}_l$ $(l = 1, \ldots, L)$, where $\boldsymbol{\epsilon}_l$ is a vector drawn from a distribution which models the pseudo-measurement noise. Before establishing the update step, intermediary matrices are defined next, which will be reused for the theoretical derivations.

$$H^* = H - \Psi H, \quad C = QH^T\Psi^T, \quad D^* = D - \Psi D \tag{3.7}$$

$$R^* = (R - \Psi R \Psi^T) + \Psi H Q H^T \Psi^T \tag{3.8}$$

The updated observation and measurement matrices (H^* and D^*, respectively, are computed in (3.7). The updated measurement error matrix R^* is computed in (3.8); Ψ is used to remove the time correlation of the forecast error between two time-steps. The model noise matrix Q is needed to ensure that the noise introduced by the evolution step is retained. Indeed such noise does not have any time correlation component. In this context, the observation matrix H is the identity matrix (in Section 3.4 the observation matrix will not be the same). The update equations for the assimilation of pseudo-measurements are given as:

$$E = H^* \text{cov}(X_p^k) H^{*T} + R^* + H^* C + C^T H^{*T} \tag{3.9}$$

$$K = (\text{cov}(X_p^k) H^{*T} + C) E^{-1} \tag{3.10}$$

$$X_u^k = X_p^k + K(D^* - H^* X_p^k) \tag{3.11}$$

3.3.4 Assimilation of PMU Measurements

Similar to the pseudo-measurements, the measurements coming from the PMUs are contained in a vector $\mathbf{z}$ of size $2|S|$. An ensemble Z of L perturbed observation vectors is computed such that $Z = [\mathbf{z}_1, \ldots, \mathbf{z}_L]$, with each $\mathbf{z}_l = \mathbf{z} + \boldsymbol{\xi}_l$ $(l = 1, \ldots, L)$, where $\boldsymbol{\xi}_k$ is a vector drawn from a distribution which models the measurement noise.

The measurements from the PMUs can be related to the state vector using a function h, such that $\mathbf{z}_l = h(\mathbf{x}_l) + \boldsymbol{\gamma}_k$, where $\boldsymbol{\gamma}_k$ is an error vector. The function $h(\cdot)$ takes as input the system state and returns a vector containing the measurements that would have been observed considering that particular system state. Given that $\mathbf{x}$ contains the active and reactive powers injected at each bus, $h(\cdot)$ is the power-flow solution; the EnKF does not need to know the analytical expression of $h(\cdot)$. It is the solution given by the LDC's power-flow solver, for example. This makes the EnKF independent of the way power-flows are computed. The cost of such independence is computational: one need to compute L power-flows at each time-step. Since $h(\cdot)$ is non-linear, the measurements cannot be obtained directly from the state using a simple multiplication by an observation matrix. Instead, $h(\mathbf{x})$ needs to be computed explicitly. A temporary augmented state $\widehat{\mathbf{x}}$ and augmented ensemble $\widehat{X}_u^k$ are used to perform the assimilation, where:

$$\widehat{\mathbf{x}}_l = [\mathbf{x_l}^T, h^T(\mathbf{x}_l)]^T, \quad \widehat{X}_u^k = [\widehat{\mathbf{x}}_1, \ldots, \widehat{\mathbf{x}}_L] \tag{3.12}$$

The updated ensemble X_a^k is then computed:

$$X_a^k = X_u^k + K(Z - \widehat{H}\widehat{X}_u^k) \tag{3.13}$$

$$K = \mathrm{cov}(X_u^k, \widehat{H}\widehat{X}_u^k)[\mathrm{cov}(\widehat{H}\widehat{X}_u^k) + \mathrm{cov}(Z)]^{-1} \tag{3.14}$$

where $\widehat{H}$ is a selection matrix used to select the rows of the state vector corresponding to the desired measurements.

3.4 Theoretical formulation

In this section, a method to compute a theoretical estimate of the performance and the improvement achieved by the proposed PASE method is developed. It is based on [26], where the authors proposed a technique for estimating a priori the performances of the WLS estimator. Their work is extended to fit the EnKF and compute the relative gain between the two. The derivation is performed under the following assumptions, also made

in [26]. The state vector is represented by $\mathbf{w} = [\underline{v}_1, \ldots, \underline{v}_{|I|}]^T$. The forecast variance, the forecast error time-correlation and load evolution model variance are assumed to be constant and identical for active and reactive powers. They are denoted respectively $(\sigma_i^f)^2$, ψ_i^f and $(\sigma_i^d)^2$. At each bus i, the apparent power magnitude $|S_i^f|$ is used to represent the load forecast. In the analysis framework, the shape of the load evolution model is not need to be known, the value of the variance is sufficient.

The theoretical computations are performed by using a linear Kalman filter. The covariance matrices are made time-invariant in order to obtain a steady-state formulation of the filter [4]. From this formulation, the covariance matrix of the system state can be computed and used to approximate the performance of the non-linear EnKF. The performance of WLS can also be computed since it can be seen as a Kalman filter that is reset for each new estimation. To evaluate the performance of the two state estimators over a period of time T, the average root mean square error of the voltage estimate (ARMSEV) is used as metric:

$$\text{ARMSEV} = \sqrt{\frac{1}{T|I|} \sum_{t=0}^{T} \sum_{i=1}^{|I|} \mathbf{E}[|\hat{\underline{v}}_i[t] - \underline{v}_i[t]|^2]} \tag{3.15}$$

where $\underline{v}_i$ is the true voltage at bus i and $\hat{\underline{v}}_i$ the estimated one. A linear version of the power-flow equations is used; it is the first iteration of backward-forward sweep. The backward-forward sweep was presented in Section 2.1.3 (page 10). The vectorized formulation is used, based on the distribution load flow matrix, denoted by M. The relationship between the injected power at each bus (represented by the vector $\mathbf{s} = [\underline{s}_1, \ldots, \underline{s}_{|I|}]^T$, with $\underline{s}_i$ the injected power at bus i) and the state vector is given as:

$$\mathbf{w} = [V_0, \ldots, V_0]^T + \frac{1}{V_0} M \times \bar{\mathbf{s}} \tag{3.16}$$

where $\bar{\mathbf{s}}$ is the conjugate of $\mathbf{s}$. Several matrices used by the Kalman equations are defined. The load evolution noise covariance matrix Q expressed in terms of the apparent power, and the forecast error covariance matrix R_S are computed as follows:

$$Q = \text{diag}((\sigma_1^d)^2, \ldots, (\sigma_{|I|}^d)^2) \tag{3.17}$$

$$R_S = \text{diag}((\sigma_1^f)^2, \ldots, (\sigma_{|I|}^f)^2) \tag{3.18}$$

The PMU measurement error covariance matrix is approximated by assuming that the variance of the voltage error when projected onto the real and imaginary axes is the same and equal to $\sigma_{PMU}^2 V_0^2$, where σ_{PMU}^2 is the relative variance of the PMU measurements such that $R_{PMU} = 2\sigma_{PMU}^2 V_0^2 \times I_{|S|}$, where $I_{|S|}$ is the $|S| \times |S|$ identity matrix.

The steady state covariance matrix of the state vector is computed by iterating the Kalman equations. The covariance matrix is denoted by $\Sigma_a^{(\cdot)}$. The iteration number is indicated in the parenthesis $(\cdot)$. Such matrix will converge to a steady state covariance matrix $\Sigma_a^{(ss)}$. For each iteration, two other matrices are used to track the covariance matrix during intermediary steps: $\Sigma_p^{(\cdot)}$ and $\Sigma_u^{(\cdot)}$. They represent respectively the covariance matrix of the prior state and the state after assimilation of PMU measurements. At iteration 0, the prior covariance matrix of the state is computed such that:

$$\Sigma_p^{(0)} = M \times R_S \times M^H \tag{3.19}$$

where $(\cdot)^H$ indicates the Hermitian transpose (transpose conjugate operator). The updated covariance matrix obtained after the assimilation of the PMU measurements is then computed:

$$\Sigma_a^{(0)} = \Sigma_p^{(0)} - KH\Sigma_p^{(0)} \tag{3.20}$$

$$K = \Sigma_p^{(0)} H^T (H\Sigma_p^{(0)} H^T + R)^{-1} \tag{3.21}$$

where H is the observation matrix for PMU measurements. It is a selection matrix that relates state variables to the measurement vector. One can estimate the ARMSEV performance of WLS based on $\Sigma_a^{(0)}$:

$$\text{ARMSEV}_{\text{WLS}} = \sqrt{\frac{1}{|I|}\text{trace}(\Sigma_a^{(0)})} \tag{3.22}$$

Any iteration it ($it \neq 0$) is performed in 3 steps: first the prior covariance matrix $\Sigma_p^{(it)}$ is computed based on the previous iteration, then the covariance matrix is updated using the PMU measurement covariance matrix, and finally the pseudo-measurements are assimilated. The first two steps are such that (where H is the same matrix as in (3.20)):

$$\Sigma_p^{(it)} = \Sigma_a^{(it-1)} + M \times Q \times M^H \tag{3.23}$$

$$\Sigma_a^{(it)} = \Sigma_p^{(it)} - KH\Sigma_p^{(it)} \tag{3.24}$$

$$K = \Sigma_p^{(it)} H^T (H\Sigma_p^{(it)} H^T + R_{PMU})^{-1} \tag{3.25}$$

The third step differs because of the pseudo-measurement error time correlation (see Section 3.3.3). The same time-differentiation method is used. The same updated matrices are computed according to (3.7)-(3.8) with only a few differences. Now H is the inverse DLF matrix, mapping the state vector to the injected power ($H = M^{-1}$). The forecast error

time correlation matrix is such that $\Psi = \text{diag}(\psi_1^f, \ldots, \psi_{|I|}^f)$. Finally, the matrix R used in (3.8) is such that $R = R_S$. The update equations thus become:

$$\Sigma_a^{(it)} = \Sigma_u^{(it)} - (\Sigma_u^{(it)}(H^*)^T + C) \times K^T \tag{3.26}$$

$$K = \begin{array}{l} [\Sigma_u^{(it)} * (H^*)^T + C] \times [H^* \Sigma_u^{(it)} (H^*)^T \\ + R^* + H^* C + C^T (H^*) T]^{-1} \end{array} \tag{3.27}$$

Once the steady state is reached after a few iterations, the theoretical performance of the EnKF can be computed. The ARMSEV error is such that:

$$\text{ARMSEV}_{\text{EnKF}} = \sqrt{\frac{1}{|I|} \text{trace}(\Sigma_a^{(ss)})} \tag{3.28}$$

The relative gain is expressed as:

$$\text{Gain} = \frac{\text{ARMSEV}_{\text{WLS}} - \text{ARMSEV}_{\text{EnKF}}}{\text{ARMSEV}_{\text{WLS}}} \tag{3.29}$$

3.5 Validation

The improvement in performance achieved by the proposed PASE method over WLS is evaluated by considering a 33-bus test distribution feeder (described Section 3.1, page 21) under normal operations. The WLS estimation problem is modeled in GAMS environment and solved using the MINOS solver. Attention has been paid to avoid potential numerical issues. The ensemble size is set to $L = 500$ and the power flow solutions obtained from $h(\cdot)$ are computed using the backward/forward sweep method [30]. The system is simulated over a period of 24 hours. For the theoretical estimation, 50 iterations ($(ss) = 50$) are enough to compute the steady-state of the state covariance matrix.

3.5.1 Description of 33-Bus Load Profiles

The 33-bus test feeder data includes active and reactive power loads at each bus; bus-1 is the substation transformer bus, with V_0 set to 12.66 kV. The number of houses n_i aggregated at a bus i is selected such that $n_i = n_{11} P_i^{33bus} / P_{11}^{33bus}$ where $n_{11} = 10$ houses

and P_i^{33bus} is the static 33-bus active power load at bus i. The number of houses aggregated at each bus can be found in table A.2 (page 47). These values were chosen in order to have a large range of aggregation levels. The corresponding distribution transformer traces are generated from the second half of the dataset, by summing the desired number of profiles, picked randomly. Each trace is then scaled so that the mean of the profile matches the load values. The values given by the empirical function in Section 3.2 are scaled accordingly. Because no dataset for reactive power consumption is available, active and reactive power profiles are generated independently from the same dataset.

3.5.2 Measurement Model

The simulation models used for measurements are described in this section.

PMU: the PMU measurement error is simulated as an additive white Gaussian noise of nominal variance σ_{PMU}^2, for both voltage magnitudes and angles. Additive white Gaussian noise is a common assumption for PMU measurement [26]. The readings $\tilde{V}_s$ and $\tilde{\delta}_s$ provided by the PMU at each bus s ($s \in S \subseteq I$) have an error variance such that $\mathbf{E}[\tilde{a}^2] = \sigma_{PMU}^2 * \tilde{a}^2$, where $\tilde{a}$ indicates either the voltage magnitude or angle. The measurement errors are independent across buses, and the voltage magnitude error independent of the angle error. The PMU resolution is set to 1% ($\sigma_{PMU} = 0.01$); the PMU placement map $\mathscr{S}$ is determined using a greedy method [26], i.e., PMUs are sequentially added at the location that provides the most improvement (with 32 load buses, a maximum of 32 PMUs). The placement of PMUs is beyond the scope of this work; many researchers have addressed this issue, see for example [29].

Pseudo-measurements: the forecasts P_i^f and Q_i^f are taken as the mean value of the load profile generated at each distribution transformer i, as in [26]. They are constant over the simulated period. Using the training set, the nominal standard deviation of the forecast was evaluated and set to $\sigma_0 = 30\%$, for both active and reactive powers, irrespective of the aggregation level. Such value is typical at the distribution level, where the standard deviation of forecast errors varies between 30% and 50%. Therefore for each bus i, $\sigma_i^{fp} = \sigma_0 P_i^f$ and $\sigma_i^{fq} = \sigma_0 Q_i^f$ (3.6). The constant apparent power forecast $|S_i^f|$ is such that $|S_i^f| = |P_i^f + jQ_i^f|$. Finally each σ_i^f (3.18) is computed as $\sigma_i^f = \sigma_0 |S_i^f|$. Pseudo-measurements with a Gaussian distribution are used as "best-guess" initial ensemble (Section 3.3.1).

Error time-correlation: ψ_i^p and ψ_i^q are evaluated as follows: since the same data is used for generating the active and reactive power profiles, ψ_i^p and ψ_i^q are equal. They are evaluated on the training set. Given an aggregation level and a time-step length, load profiles are built. The autocorrelation function R_i^e of the difference between the profile and

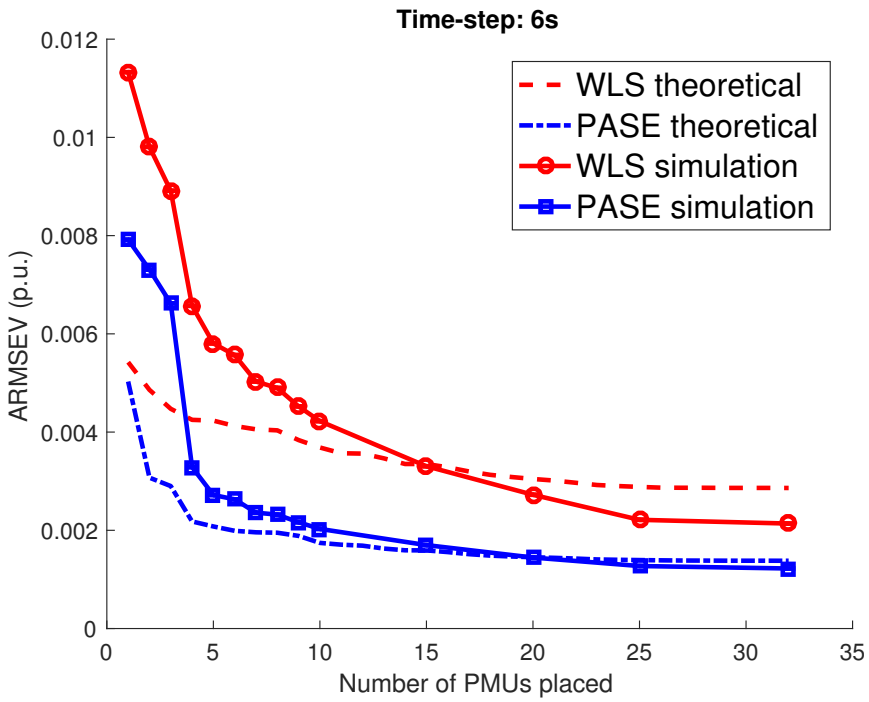

Figure 3.4: ARMSEV value function of the number of PMUs. The performance of the proposed PASE method is compared with WLS. The theoretical results are also compared against simulation results. A lower value means better performance.

its mean (representing the forecast error) is computed. The value of ψ_i^p and ψ_i^q is given by $R_i^e(\Delta T)$.

3.5.3 Validation

The theoretical and simulation results are presented in Figs. 3.4-3.6, obtained by averaging the results of several realizations. A realization is defined as the observed performance of both the WLS and PASE on the 33-bus system. For each realization, new load profiles are generated based on the testing set, while the other parameters stay the same. The performance of the WLS and PASE are plotted alongside with the theoretical ones in Fig. 3.4, where a time-step of 6 seconds has been used. WLS has been studied in [26] using synthetic data. Similar trends are observed here with real data. Note that since WLS is snapshot-based, the size of the time-step does not matter. For PASE, the theoretical results are close to the actual performance observed in simulation as the number of PMUs

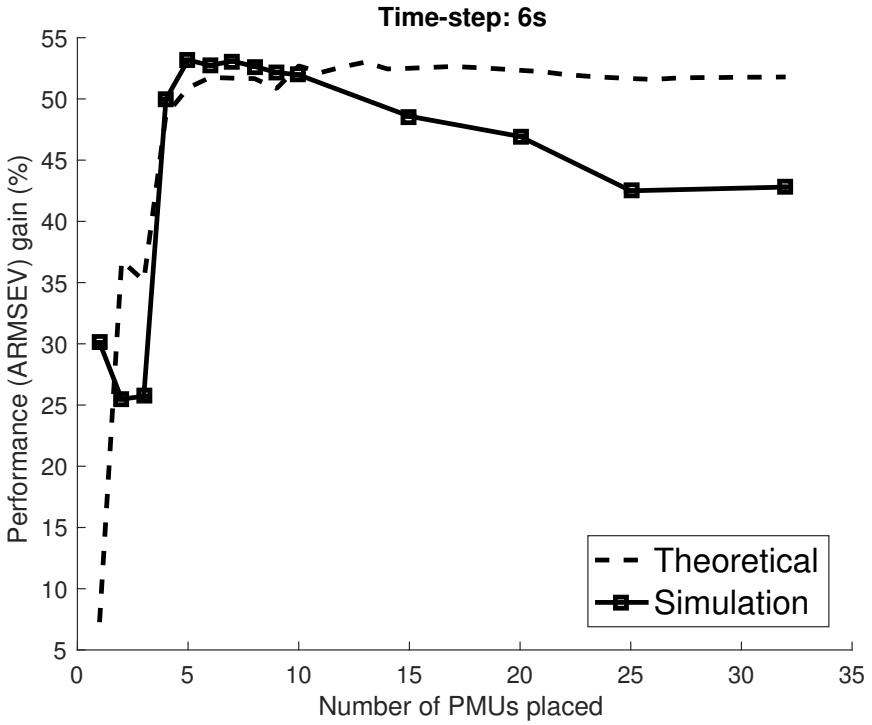

Figure 3.5: Comparison of the gain from using PASE over WLS on ARMSEV depending on the number of PMUs. The theoretical results are compared to the observed gain in simulation.

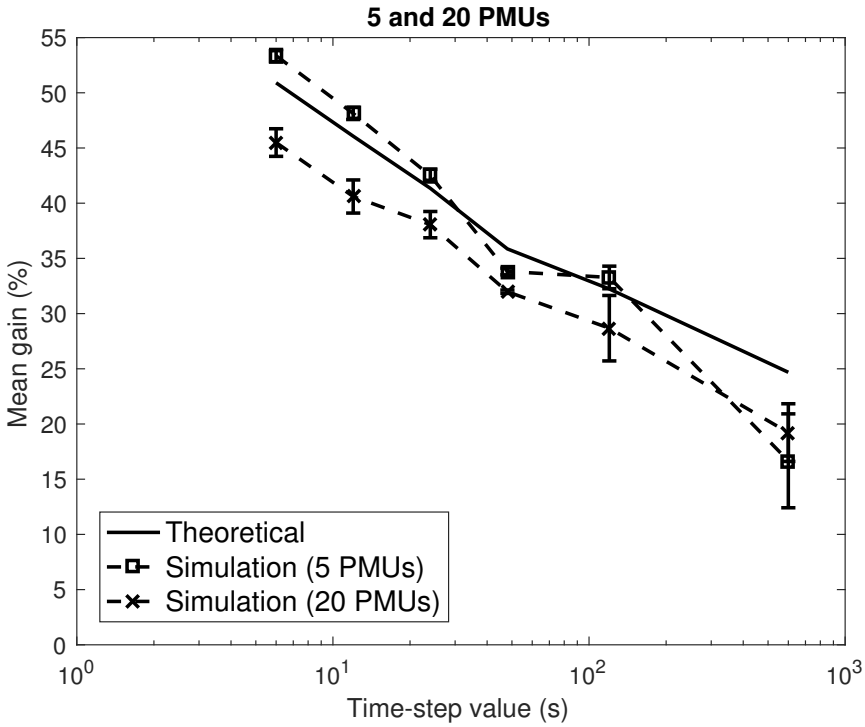

Figure 3.6: Influence of the time-step on the mean performance gain. The theoretical results are compared to the observed gain in simulation. The time-step axis has a logarithmic scale. The error bars represent the standard deviation. The 5 PMUs are placed at buses [17, 18, 31, 32, 33]. The 20 PMUs are placed at buses [7-18, 26-33]

introduced in the system increases, which validates the theoretical approach. Similar trends are observed for different time-steps. The actual gain brought about by PASE is compared with the theoretical one in Fig. 3.5 for a time step of 6 seconds. Finally the influence of the time-step on the gain is compared in Fig. 3.6 for two PMU configurations (5 PMUs and 20 PMUs). Theory and simulation follow the same trend. The gap between theory and simulation is relative to that observed in Fig. 3.5. For 5 PMUs, a separation between the curves is observed.

3.5.4 Comparison Between WLS and Proposed PASE Method

The results presented in Fig. 3.4 illustrate the improvements achieved by the proposed PASE method. Clearly, using a load evolution model improves the performance of the estimator; given an arbitrary target error of 0.004 p.u., WLS requires more than 10 PMUs while PASE only 4. Even when each bus of the distribution system is monitored by a PMU, the proposed PASE method still brings about an improvement of more than 40% when using a time-step of 6 seconds. As illustrated in Fig. 3.6, higher gains are obtained for smaller time-steps. Indeed, for larger time-steps, the load has more chances of changing by a large magnitude between two estimates and thus has less inertia. Even for large time-step (e.g., 10 mins) there is a gain of about 15%. In practice, the granularity of the time-step depends on the available computational speed. The smallest time-step considered in this work is 6 seconds and represents a lower-bound on what was tried out. In comparison, the DSSE problem was solved at each step in under 1 second. For larger systems, solving a power-flow problem requires more computational power, hence the overall computational cost of the method will be higher. However, the power-flow problems can easily be parallelized with PASE.

3.5.5 Engineering Insights

In practice, the LDC will need to make trade-offs in the choice of the following parameters: number of PMUs, their accuracy and the time scale. The influence of PMU accuracy on the theoretical gain achieved by PASE is shown in Fig. 3.7, the three parameters considered are depicted in the plot. The maximum gain is attained for a PMU error variance of about 1%. Clearly as the PMU measurement standard deviation decreases (i.e., the PMU becomes more and more accurate) the gain achieved by PASE decreases since the load evolution model is not as useful in such circumstances. Similarly, as the standard deviation of the PMU increases, the gain decreases, since the load evolution model has to compensate

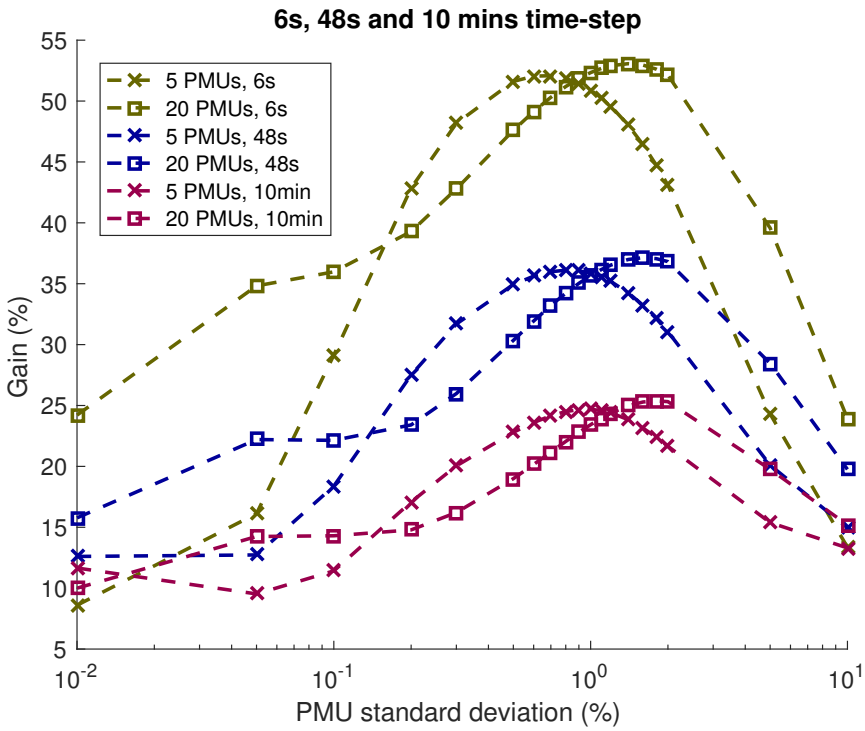

Figure 3.7: Influence of PMU quality on the (theoretical) gain achieved by PASE over WLS. The PMU accuracy is characterized by its measurement error standard deviation, a lower value means a more accurate PMU. A logarithmic scale is used for the variance axis.

for both poor forecast accuracy and poor PMU measurement accuracy. This figure also illustrates the role of the time-step, the gain achieved by the filtering technique decreasing as the time-step increases, underlining the limits of the load evolution model.

The trade-off between the three parameters considered is illustrated by Fig. 3.8: two PMU accuracies are used to draw the plots. An arbitrary target error is fixed and the minimum number of PMUs required is determined as a function of the time-step. Clearly, the time-step has little influence on a very accurate PMU. However, the more accurate the PMU, the more costly it will be. With the same number of PMUs placed in the system (4), choosing a PMU ten times less accurate will provide the same performance given that a time-step small enough (6 seconds) is chosen.

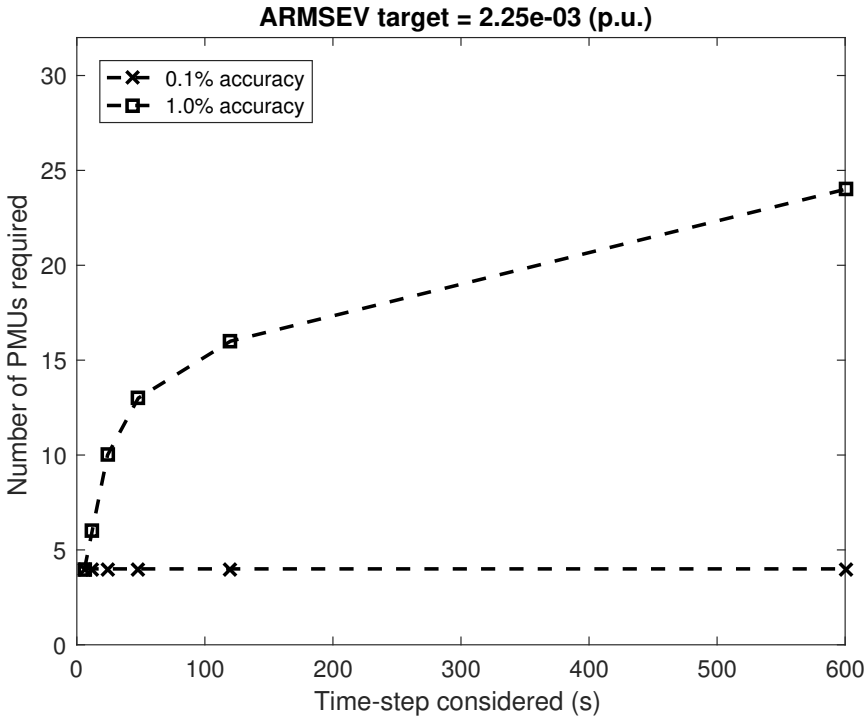

Figure 3.8: Minimum number of PMUs required to achieve an average target error of $2.25e-3$ p.u., function of time-step and for two PMU accuracies (computed using the theoretical formulation).

Chapter 4

Conclusions and Future Work

4.1 Contributions

In this work, a novel PASE method for DSSE and its analysis framework were presented. A simple load evolution model for characterizing aggregate load changes at a distribution transformer was derived. The method used for obtaining the model is versatile and can be applied to any dataset. The proposed PASE method was compared to WLS and validated using real power consumption data. PASE does not embed the power-flow equations in its formulation and instead relies on an external power-flow solver, which makes the solution very flexible. The PASE method performs the fusion of measurements and pseudo-measurements and requires fewer PMUs than WLS to achieve the same estimation error, for time-steps under 15 minutes. Engineering insights were presented highlighting the major trade-offs in the choice of decision variables for the LDC. Using a smaller time-step allows the LDC to relax the requirements on the PMU quality and their number.

4.2 Future work

There are several remaining challenges to tackle. The influence of distributed generation on state estimation and its modeling is a compelling one. Likewise, the effects of electric vehicle charging are an interesting topic. It would also be worthwhile studying the impact of an unbalanced system on PASE; given that PASE uses an external power-flow solver, most of the work would probably be handled by the solver. Finally, studying the differences in terms of load evolution models between different regions of the globe is an enticing

future direction, as more and more fine-grained power consumption datasets are being collected around the world. Similarly, the performances of PASE could be appraised on those dataset.

References

[1] Normal Equations. In *The Concise Encyclopedia of Statistics*, pages 380–382. Springer New York, 2008.

[2] OpenDSS, 2017. Available at https://sourceforge.net/p/electricdss/wiki/Home/.

[3] S.M.S. Alam, B. Natarajan, and A. Pahwa. Distribution Grid State Estimation from Compressed Measurements. *IEEE Trans. Smart Grid*, 2014.

[4] BDO Anderson and JB Moore. *Optimal Filtering*. Prentice-Hall, 1979.

[5] O. Ardakanian, S. Keshav, and C. Rosenberg. Real-Time Distributed Control for Smart Electric Vehicle Chargers: From a Static to a Dynamic Study. *IEEE Trans. Smart Grid*, 2014.

[6] Omid Ardakanian, Srinivasan Keshav, and Catherine Rosenberg. Markovian Models for Home Electricity Consumption. In *ACM SIGCOMM*, 2011.

[7] A. Arefi, G. Ledwich, and B. Behi. An Efficient DSE Using Conditional Multivariate Complex Gaussian Distribution. *IEEE Transactions on Smart Grid*, 6(4):2147–2156, July 2015.

[8] D. Atanackovic and V. Dabic. Deployment of real-time state estimator and load flow in BC Hydro DMS - challenges and opportunities. In *2013 IEEE Power Energy Society General Meeting*, 2013.

[9] M. E. Baran and A. W. Kelley. State estimation for real-time monitoring of distribution systems. *IEEE Transactions on Power Systems*, 9(3):1601–1609, August 1994.

[10] M. E. Baran and F. F. Wu. Network reconfiguration in distribution systems for loss reduction and load balancing. *IEEE Trans. on Power Del.*, 1989.

[11] Geir Evensen. The Ensemble Kalman Filter: theoretical formulation and practical implementation. *Ocean Dynamics*, 53, November 2003.

[12] C. A. Fantin, M. R. C. Castillo, B. E. B. de Carvalho, and J. B. A. London. Using pseudo and virtual measurements in distribution system state estimation. In *IEEE PES T&D-LA*, 2014.

[13] M. B. Do Coutto Filho and J. C. Stacchini de Souza. Forecasting-Aided State Estimation - Part I: Panorama. *IEEE Trans. on Power Systems*, 2009.

[14] A. K. Ghosh, D. L. Lubkeman, M. J. Downey, and R. H. Jones. Distribution circuit state estimation using a probabilistic approach. *IEEE Transactions on Power Systems*, 1997.

[15] D. A. Haughton and G. T. Heydt. A Linear State Estimation Formulation for Smart Distribution Systems. *IEEE Trans. on Power Systems*, 2013.

[16] Shih-Che Huang, Chan-Nan Lu, and Yuan-Liang Lo. Evaluation of AMI and SCADA Data Synergy for Distribution Feeder Modeling. *IEEE Trans. Smart Grid*, 2015.

[17] A. S. B. Humayd, B. Lami, and K. Bhattacharya. The effect of PEV uncontrolled and smart charging on distribution system planning. In *2016 IEEE Electrical Power and Energy Conference (EPEC)*, pages 1–6, October 2016.

[18] Rudolph Emil Kalman. A new approach to linear filtering and prediction problems. *Journal of basic Engineering*, 82(1), 1960.

[19] C. Klauber and H. Zhu. Distribution system state estimation using semidefinite programming. In *NAPS*, 2015.

[20] A. Monticelli. *State Estimation in Electric Power Systems*. Springer, 1999.

[21] S. Paudyal, C. A. Canizares, and K. Bhattacharya. Optimal Operation of Distribution Feeders in Smart Grids. *IEEE Transactions on Industrial Electronics*, 2011.

[22] M. G. Petovello, K. OKeefe, G. Lachapelle, and M. E. Cannon. Consideration of time-correlated errors in a Kalman filter applicable to GNSS. *Journal of Geodesy*, 2009.

[23] A. Primadianto and C. N. Lu. A Review on Distribution System State Estimation. *IEEE Transactions on Power Systems*, 2016.

[24] R. N. Rodrigues, J. K. Zatta, P. C. C. Vieira, and L. C. M. Schlichting. A low cost prototype of a Phasor Measurement Unit using Digital Signal Processor. In *IEEE Biennial Congress of Argentina*, June 2016.

[25] Stela Sarri, Mario Paolone, Rachid Cherkaoui, Alberto Borghetti, Fabio Napolitano, and Carlo Alberto Nucci. State estimation of active distribution networks: comparison between WLS and iterated Kalman-filter algorithm integrating PMUs. In *Innovative Smart Grid Technologies (ISGT Europe)*, 2012.

[26] L. Schenato, G. Barchi, D. Macii, R. Arghandeh, K. Poolla, and A. Von Meier. Bayesian linear state estimation using smart meters and PMUs measurements in distribution grids. In *SmartGridComm*, 2014.

[27] Raffi Sevlian and Ram Rajagopal. Short term electricity load forecasting on varying levels of aggregation. *arXiv preprint arXiv:1404.0058*, 2014.

[28] R. Singh, B. C. Pal, and R. A. Jabr. Choice of estimator for distribution system state estimation. *IET Gener. Transm. Distrib.*, 2009.

[29] R. Singh, B. C. Pal, and R. B. Vinter. Measurement Placement in Distribution System State Estimation. *IEEE Trans. on Power Syst.*, 2009.

[30] Jen-Hao Teng. A direct approach for distribution system load flow solutions. *IEEE Transactions on Power Delivery*, July 2003.

[31] A. von Meier, D. Culler, A. McEachern, and R. Arghandeh. Micro-synchrophasors for distribution systems. In *ISGT, IEEE PES*, 2014.

[32] R.A. Walling, R. Saint, R.C. Dugan, J. Burke, and L.A. Kojovic. Summary of Distributed Resources Impact on Power Delivery Systems. *IEEE Transactions on Power Delivery*, July 2008.

[33] Haibin Wang and N. N. Schulz. A revised branch current-based distribution system state estimation algorithm and meter placement impact. *IEEE Transactions on Power Systems*, 19(1):207–213, February 2004.

[34] K. Wang, Y. Li, and C. Rizos. Practical Approaches to Kalman Filtering with Time-Correlated Measurement Errors. *IEEE Trans. Aerosp. Electron. Syst.*, 2012.

[35] Zhian Zhong. *Power systems frequency dynamic monitoring system design and applications*. PhD thesis, Virginia Polytechnic Institute and State University, 2005.

APPENDICES

Appendix A

Distribution System Data

A.1 33-Bus system

Table A.1: Feeder parameters for 33-Bus system

Line	R (ohms)	X (ohms)	Charging (p.u.)
Main branch			
1.2	0.0922	0.0477	0.0052
2.3	0.493	0.2511	0.0277
3.4	0.366	0.1864	0.0206
4.5	0.3811	0.1941	0.0214
5.6	0.819	0.707	0.046
6.7	0.1872	0.6188	0.0105
7.8	0.7114	0.2351	0.0961
8.9	1.03	0.74	0.0578
9.1	1.044	0.74	0.0586
10.11	0.1966	0.065	0.011
11.12	0.3744	0.1238	0.021
12.13	1.468	1.155	0.0824
13.14	0.5416	0.7129	0.0304
14.15	0.591	0.526	0.0332
15.16	0.7463	0.545	0.0419
16.17	1.289	1.721	0.0724
17.18	0.732	0.574	0.0411
Branch 1			
2.19	0.164	0.1565	0.0092
19.2	1.5042	1.3554	0.0845
20.21	0.4095	0.4784	0.023
21.22	0.7089	0.9373	0.0398
Branch 2			
3.23	0.4512	0.3083	0.0253
23.24	0.898	0.7091	0.0504
24.25	0.896	0.7011	0.0503
6.26	0.203	0.1034	0.0114
26.27	0.2842	0.1447	0.016
27.28	1.059	0.9337	0.0595
28.29	0.8042	0.7006	0.0452
29.3	0.5075	0.2585	0.0285
30.31	0.9744	0.963	0.0547
31.32	0.3105	0.3619	0.0174
32.33	0.341	0.5302	0.0191

Table A.2: Load data for 33-Bus system

Bus (i)	P (kW)	Q (kW)	Simulated number of houses
2	100	60	23
3	90	40	20
4	120	80	27
5	60	30	14
6	60	20	14
7	200	100	45
8	200	100	45
9	60	20	14
10	60	20	14
11	45	30	10
12	60	35	14
13	60	35	14
14	120	80	27
15	60	10	14
16	60	20	14
17	60	20	14
18	90	40	20
19	90	40	20
20	90	40	20
21	90	40	20
22	90	40	20
23	90	50	20
24	420	200	94
25	420	200	94
26	60	25	14
27	60	25	14
28	60	20	14
29	120	70	27
30	200	600	45
31	150	70	34
32	210	100	47
33	60	40	14